Mineralium Deposita (2018) 53:1213–1230
https://doi.org/10.1007/s00126-018-0802-8

ARTICLE

Genesis of copper-lead mineralization in the regionally zoned Agnigundala Sulfide Belt, Cuddapah Basin, Andhra Pradesh, India

H. N. Bhattacharya[1] · Sandip Bandyopadhyay[2]

Received: 27 June 2017 / Accepted: 19 March 2018 / Published online: 28 March 2018

Abstract

Shallow marine sandstone-shale-carbonate sedimentary rocks of the Paleoproterozoic northern Cuddapah basin host copper (Nallakonda deposit), copper-lead (Dhukonda deposit), and lead mineralization (Bandalamottu deposit) which together constitute the Agnigundala Sulfide Belt. The Cu sulfide mineralization in sandstone is both stratabound and disseminated, and Pb sulfide mineralization occurs as stratabound fracture filling veins and/or replacement veins within dolomite. Systematic mineralogical and sulfur, carbon, and oxygen isotope studies of the three deposits indicate a common ore-fluid that deposited copper at Nallakonda, copper-lead at Dhukonda, and lead at Bandalamottu under progressive cooling during migration through sediments. The ore-fluid was of low temperature (< 200 °C) and oxidized. Thermochemical reduction of basinal water sulfate produced sulfide for ore deposition. It is envisaged that basal red-bed and evaporite-bearing rift-related continental to shallow marine sediments might have acted as the source for the metals. Rift-related faults developed during sedimentation in the basin might have punctured the ore-fluid pool in the lower sedimentary succession and also acted as conduits for their upward migration. The ore-bearing horizons have participated in deformations during basin inversion without any recognizable remobilization.

Keywords Paleoproterozoic · Cuddapah basin · Agnigundala Sulfide Belt · Cu-Pb sulfides

Introduction

Proterozoic intracontinental rift basins are the major repository of sediment-hosted base metal sulfide deposits (Piranjo 2000; Hitzman et al. 2005; Selley et al. 2005). The Kadaro-Udokan basin of Siberia (Volodin et al. 1994), Mt. Isa-McArthur basin of Australia (Large et al. 2004), Selwyn and Belt-Purcell basins of Canada (Goodfellow 2004; Lydon 2004), and Katangan basin of Central Africa (McGowan et al. 2003; Selley et al. 2005) are some examples of well-studied Proterozoic basins with rich base metal sulfide deposits. Proterozoic intracontinental rift basins in India are also well known for their Pb-Zn-Cu sulfide ore mineralization (Sarkar and Gupta 2012). The Cuddapah basin of southern India (Fig. 1a), a Paleoproterozoic intracontinental rift basin, hosts a number of copper-lead sulfide deposits of economic to subeconomic importance (Nagaraja Rao et al. 1987).

The Agnigundala Sulfide Belt in the northeastern extremity of the Cuddapah basin represents a well-developed sediment-hosted, regionally zoned, copper-lead sulfide district with insignificant zinc content (Fig. 1a). The regional zoning is comparable to other well-studied MVT deposits like Vibernum Trend deposits of Southeast Missouri, USA; Irish Midland deposits; sediment-hosted Pb-Zn deposits of Western Australia; and some Zambian copper deposits (Leach et al. 2005 and references therein). The Agnigundala Sulfide Belt (Fig. 2a) consists of copper mineralization at Nallakonda, copper-lead mineralization at Dhukonda, and lead mineralization at Bandalamottu. This belt shows a combination of 'sediment-hosted copper sulfide deposits' of Kirkham (1989) and

Editorial handling: D. Huston

Electronic supplementary material The online version of this article (https://doi.org/10.1007/s00126-018-0802-8) contains supplementary material, which is available to authorized users.

✉ H. N. Bhattacharya
hbaruamu@gmail.com

Sandip Bandyopadhyay
banerjeesandip18@gmail.com

[1] Techno India University, West Bengal, EM-IV, Sector-5, Salt Lake, Kolkata 700091, India

[2] Department of Geology, Hooghly Mohsin College, Chinsurah, Hooghly, West Bengal, India

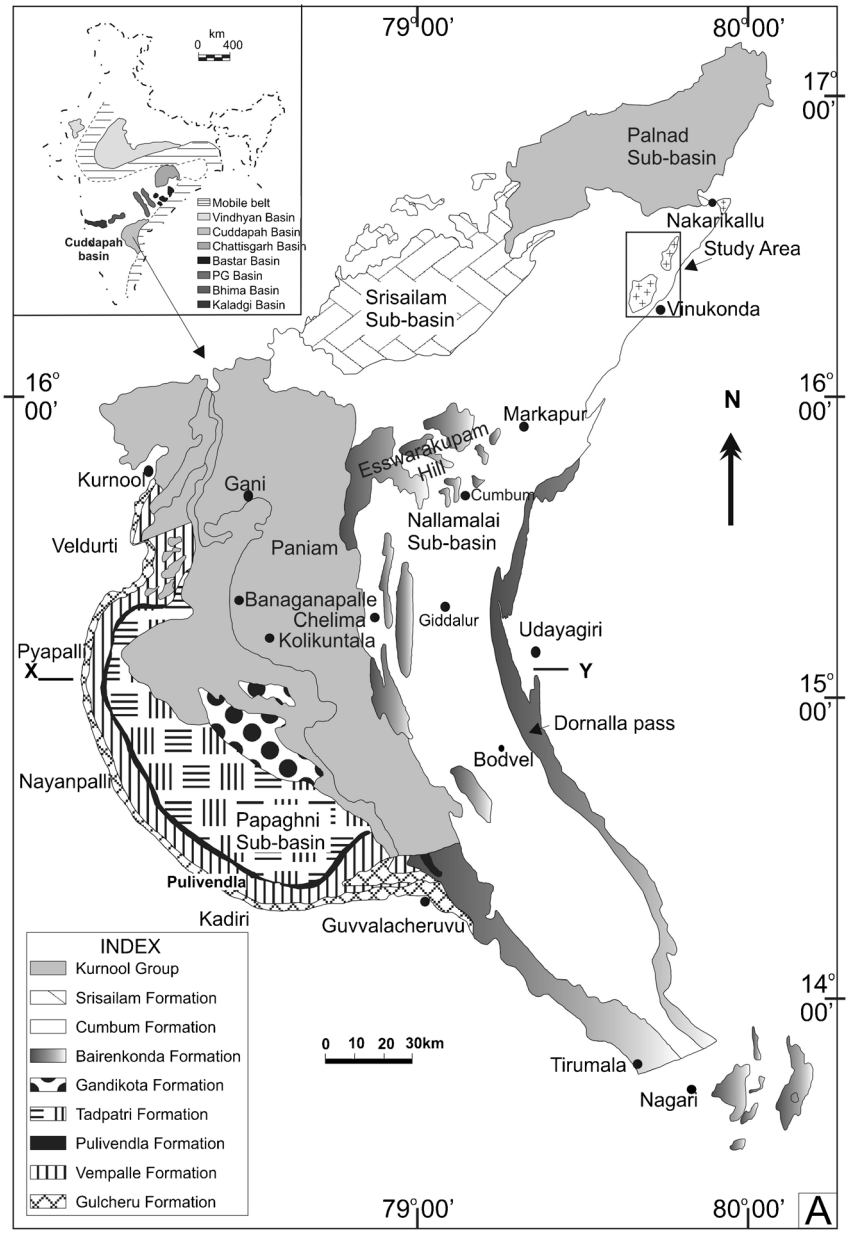
79°00'
80°00'
17° 00'
16° 00'
15° 00'
14° 00'
N
km
0 400
Mobile belt
Vindhyan Basin
Cuddapah Basin
Chattisgarh Basin
Bastar Basin
PG Basin
Bhima Basin
Kaladgi Basin
Cuddapah basin
Palnad Sub-basin
Nakarikallu
Study Area
Vinukonda
Srisailam Sub-basin
Markapur
Esswarakupam Hill
Cumbum
Nallamalai Sub-basin
Kurnool
Gani
Veldurti
Paniam
Banaganapalle
Chelima
Kolikuntala
Giddalur
Udayagiri
Pyapalli
X
Y
Dornalla pass
Bodvel
Nayanpalli
Papaghni Sub-basin
Pulivendla
Kadiri
Guvvalacheruvu
Tirumala
Nagari
0 10 20 30km
INDEX
Kurnool Group
Srisailam Formation
Cumbum Formation
Bairenkonda Formation
Gandikota Formation
Tadpatri Formation
Pulivendla Formation
Vempalle Formation
Gulcheru Formation
A

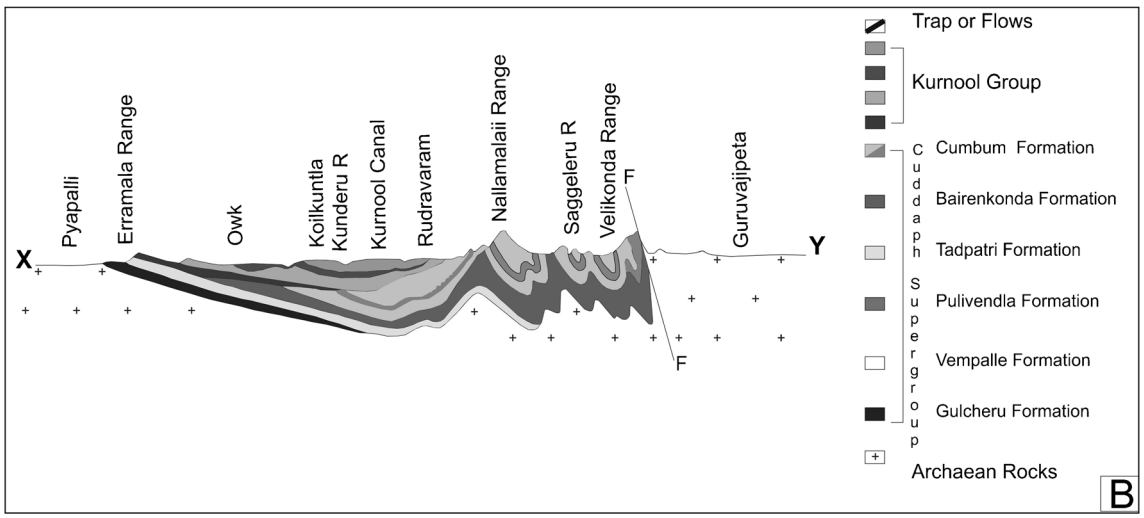
X
Y
Pyapalli
Erramala Range
Owk
Koilkuntla
Kunderu R
Kurnool Canal
Rudravaram
Nallamalaii Range
Saggeleru R
Velikonda Range
F
F
Guruvajipeta
Trap or Flows
Kurnool Group
Cumbum Formation
Bairenkonda Formation
Tadpatri Formation
Pulivendla Formation
Vempalle Formation
Gulcheru Formation
Cuddaph Supergroup
Archaean Rocks
B

◀ **Fig. 1** **a** A generalized geological map of the Cuddapah basin, showing the different lithounits (modified after Lakshminarayana et al. 2001). The study area in the northeastern extremity is a part of Cumbum Formation within the Nallamalai Fold Belt. **b** A schematic cross section of the Cuddapah basin along an east-west line through the central part of the belt (marked X-Y in **a**)

carbonate-hosted breccia-filling and replacement vein-type lead deposits.

So far as the 'sediment-hosted sulfide deposits' of different parts of the world are concerned, diverse opinions exist regarding the timing of mineralization with respect to the formation of host rocks. Proposed models include syngenetic (Garlick 1961) to early diagenetic (Brown 1974, 1978; Sweeney et al. 1986) to epigenetic (Brown 1974; Unrug 1988; Annels 1989; McGowan et al. 2003). Evaluation of the nature of the ore-fluid through fluid inclusion studies is not possible in most cases due to the fine-grained texture of the ore and gangue minerals. There is an emerging trend of convergence in the modeling of such deposits that envisages intrabasinal origin and migration of the ore-fluid, and their emplacement in rift-cover or syn-rift sediments during basin inversion (Piranjo 2000; McGowan et al. 2003; Hitzman et al. 2005; Selley et al. 2005; Hitzman et al. 2010). This paper aims to reconstruct a comprehensive deposit model of the Agnigundala Sulfide Belt through sedimentological, structural, mineralogical, and stable isotope studies of the three constituent deposits.

Cuddapah basin

The Cuddapah Supergroup represents a Paleo- to Mesoproterozoic (1800–1575 Ma: Crawford and Compston 1973) sedimentary basin that formed in an intracontinental rift system (Crawford and Compston 1973; Nagaraja Rao et al. 1987; Saha 2002; Saha and Chakraborty 2003). Extension-related block faulting in Archean granite-greenstone basement (Kaila et al. 1979; Kaila and Tewari 1985) underlying the Cuddapah basin controlled the sediment dispersal pattern. The eastern margin of the Cuddapah basin (Fig. 1b) is truncated by a thrust across which Archean rocks overrode the Cuddapah basin (Meijerink et al. 1984). The sediments and

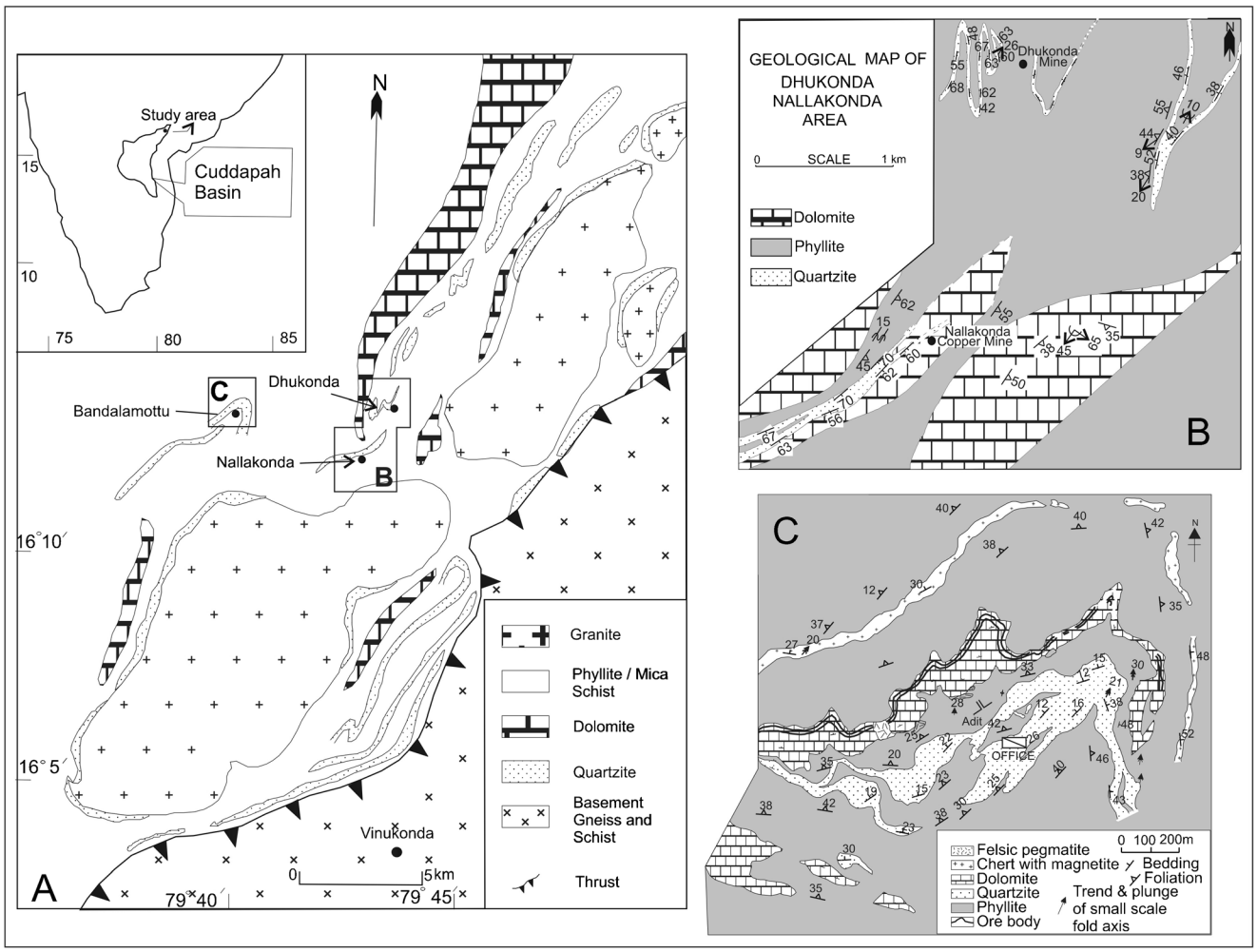

Fig. 2 **a** Geological map of the Agnigundala Sulfide Belt. **b** Geological map of Nallakonda-Dhukonda area. **c** Geological map of Bandalamottu area

intercalated volcanics are undeformed in the west but intensely deformed near the eastern margin. The litho-succession of the Cuddapah Supergroup is subdivided into two main facies sequences (Nagaraja Rao et al. 1987). The lower sequence is represented by a continental red-bed succession of conglomerate-sandstone-shale and shallow marine sandstone-shale-carbonates with or without evaporites that are intercalated with volcanic rocks. The upper sequence is represented by shallow marine carbonate-shale-calcareous shale and sandstone succession with thin intercalation of pyroclastics (Lakshminarayana et al. 2001). The lower succession, which is characterized by abrupt facies changes, is a syn-rift facies sequence deposited during the most active stages of extension and subsidence (Lakshminarayana et al. 2001). The presence of evaporites in this succession (Phansalkar et al. 1991) reflects sedimentation during low sea-level stands and scavenging of calcium from basinal volcanic flows by circulating sea water (cf. Hitzman et al. 2010).

The upper succession is a post-rift or rift-sag facies sequence deposited during the thermal subsidence phase of basin evolution (Lakshminarayana et al. 2001). As the younger sedimentary rocks directly overlie the basement, enlargement of the Cuddapah basin with time is envisaged (Chaudhuri et al. 2002). Sedimentation in the Cuddapah basin terminated as the basement granite gneiss, and the Nellore Greenstone Belt rocks overrode the sediments to form Nallamalai Fold Belt in the east (Saha 2002; Saha and Chakraborty 2003) around 1575 Ma (the age of the syn- to post-kinematic Vellaturu and Ipur granites according to Crawford and Compston 1973). Collins et al. (2015), using detrital zircon U-Pb (LA-ICP-MS) and Lu/Hf isotope data, bracketed the depositional age of Nallamalai Group between 1659 ± 22 and ~ 1590 Ma. The stratigraphic succession of the sedimentary units (formations) with interpretation in terms of environment of deposition is summarized in ESM Table 1.

Similar rift-cover sequences have been reported as host rocks for many sediment-hosted sulfide deposits the world over (Plimer 1986; Sawkins 1989; Plumb et al. 1990; Blake and Stewart 1992; O'Dea and Lister 1997; Huston et al. 2006, 2016). However, there are few cases where the rift-fill sequences host the mineralization (Lydon 2004; Bhattacharya and Bull 2010).

Agnigundala Sulfide Belt

The Agnigundala Sulfide Belt occurs near the northeastern tip of the Cuddapah basin and forms a part of the Cumbum Formation of Nallamalai Group constituting the Nallamalai Fold Belt (Fig. 1a). Shale (now phyllites) with interbedded sandstones (now quartzites) and dolomites, representing the post-rift sediments, is the main litho-types of the mineralized belt (Fig. 2a). The red-bed-bearing lower volcano-sedimentary succession, which is buried under the post-rift sediments, is not exposed in the mineralized belt. The rocks of the belt are multiply deformed and witnessed low-grade greenschist facies metamorphism. The deformation and metamorphism is coeval with the thrust lying in the east along the margin of the Cuddapah basin (Narayanswami 1966; Kaila and Tewari 1982; Chatterjee et al. 2000; Saha 2002; Saha and Chakraborty 2003). The rocks are intruded by ~ 1575 Ma syn- to post-kinematic Ipuru-Vellaturu granite bodies (Rb-Sr model age of Crawford and Compston 1973).

Three important localities in the Agnigundala Sulfide Belt (Fig. 2a) where Cu-Pb sulfide mineralization has attained economic importance are Nallakonda (3.5 Mt at 1.82% Cu), Dhukonda (2.6 Mt at 1.6% Cu and 0.5 Mt at 8.98% Pb), and Bandalamottu (10 Mt at 6.6% Pb) (Sivadas et al. 1985). All three deposits have undergone multiple phases of deformation, as indicated by the presence of multiple structural fabrics. The local stratigraphy of the deposits differs according to the relative abundance of different rock types.

Regionally developed folding in the Nallakonda area is defined by the quartzite bands and forms doubly plunging, tight, and overturned folds (Fig. 2b). The map-scale folds on quartzite at Dhukonda are either tight isoclinal or reclined with younging direction toward the core of the folds (Fig. 2b). The regional fold of the Bandalamottu mine area is a second-generation overturned fold developed on bedding and early foliation. Late subhorizontal folds are developed on the western limb of the fold (Fig. 2c). A fracture cleavage, developed at high angle to both bedding and early foliation planes, is axial planar to the late folds. These foliations are best developed within the dolomites.

A generalized cross section of the regional structural pattern (Fig. 3) reveals that the intensity of the thrust-related deformation decreases from the east to the west (Chatterjee et al. 2000). The tight reclined folds near the eastern shear contact gradually become overturned toward the Bandalamottu area. In both the Dhukonda and Nallakonda areas, the tight isoclinal to reclined folds with younging toward core are developed in the lower limb of a regionally developed westerly closing nappe structure (Fig. 3). The Bandalamottu fold is an overturned anticlinal fold whose eastern limb is straight and maintains parallelism with the attitude of the thrust plane of the eastern contact (Fig. 3). The western limb of the Bandalamottu fold, making an obtuse angle with the thrust plane, is further deformed, with development of subhorizontal folds. Near the eastern contact, the younger granites (Ipur Granite) are emplaced along the axial zone of the anticlinal structure (Fig. 3).

Host sediments and depositional setting

Despite polyphase deformation and low greenschist facies metamorphism, the sediments of Agnigundala Sulfide Belt

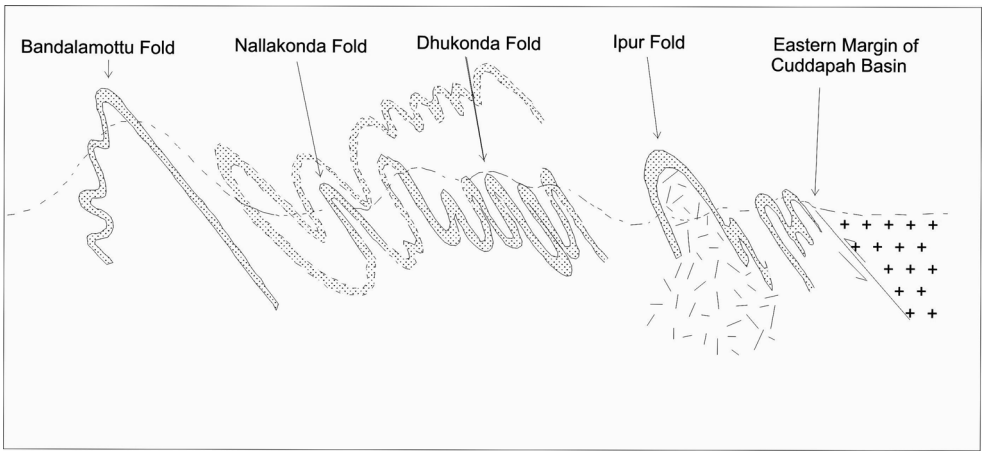

Fig. 3 A generalized cross section of Agnigundala Sulfide Belt depicting the regionally developed westerly closing nappe structure. Constructed on the basis of attitude of bedding and primary sedimentary attributes of sandstone bands. Younger granite (Ipur Granite) is emplaced along the core of the Ipur anticlinal fold. Archean basement rock overrode the Cuddapah rocks across the basin marginal thrust in the east

have retained many of their primary characteristics and are still amenable for sedimentological analysis. The succession in the studied area (Fig. 4) comprises 20-m- to more than 100-m-thick mudstone intercalated with 10- to 50-m-thick sandstone and dolomite units. The sedimentary units show lateral facies variation.

Several multistoried sandstone bodies are present in the study area and contain well-preserved primary sedimentary structures. The sandstones are trough cross-stratified (Fig. 5a) with the size of the troughs decreasing toward the top of the sandstone beds. The grain size of the sandstone units also decreases upward from very coarse sand to fine sand. In

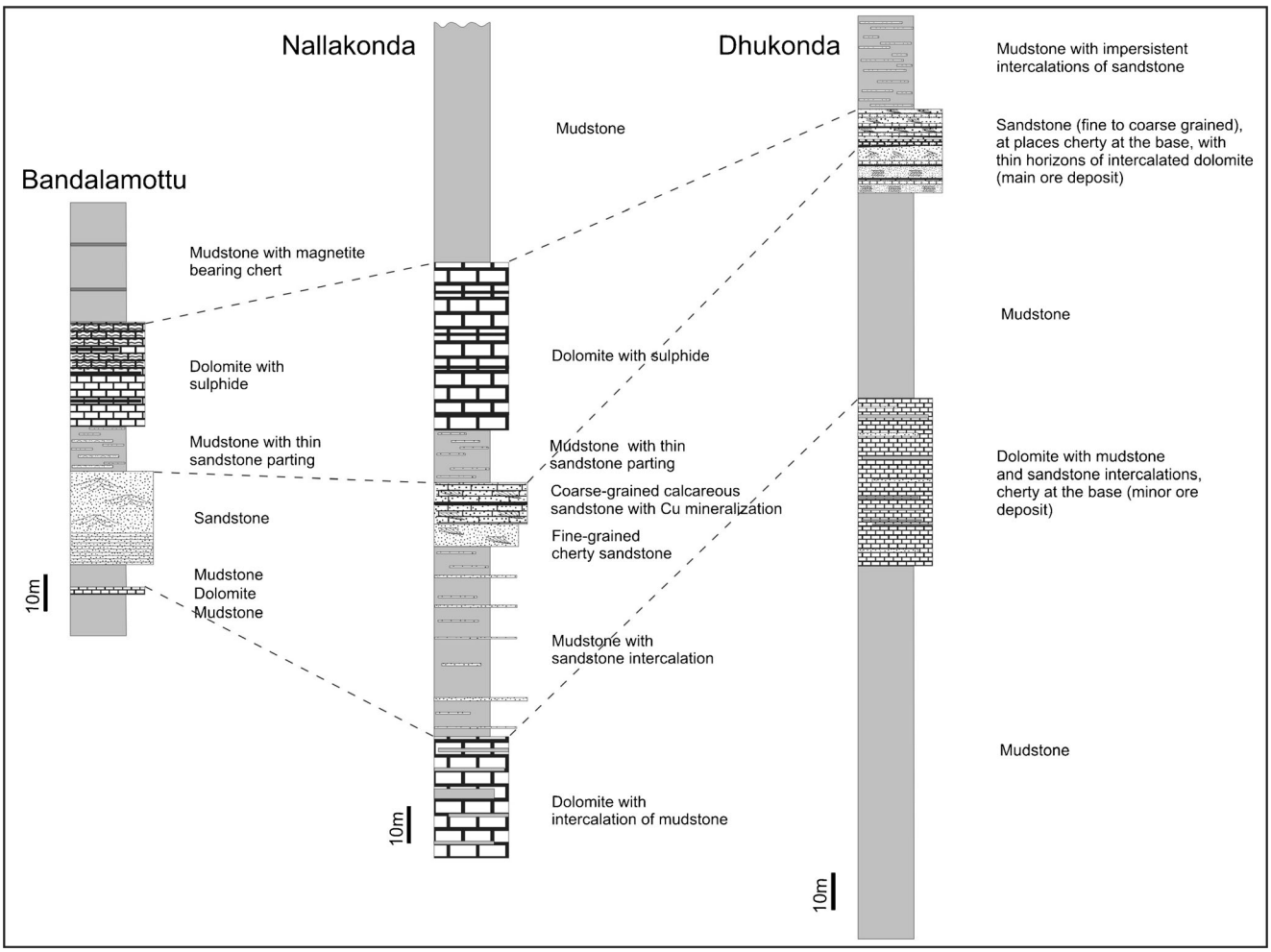

Fig. 4 Lithology of Dhukonda, Nallakonda, and Bandalamottu deposits and their correlation

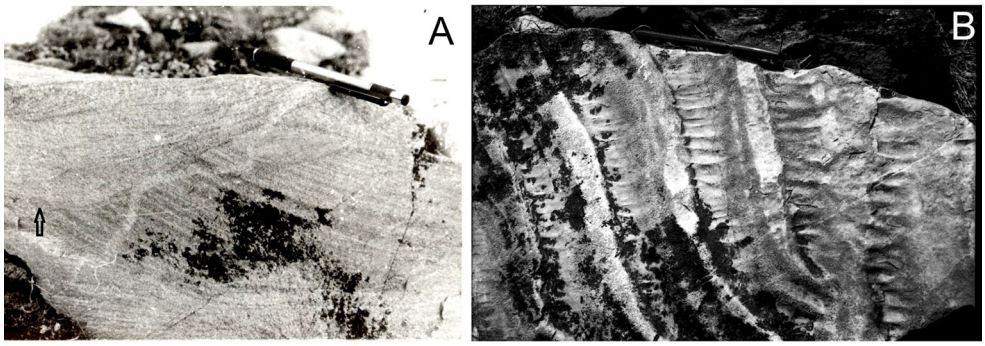

Fig. 5 Field photograph of sandstones of Dhukonda deposit. **a** Trough cross-stratification in sandstone with upward (arrow marked) decreasing trough sizes. Pen size 14.2 cm. **b** Wave ripples with sinuous flat topped crests. Note ladder back ripples along the troughs between wave ripples. Pen size 16 cm

most of the cases, foresets are bounded by reactivation surfaces. Apart from trough cross stratification, the sandstone bed at Dhukonda is also characterized by symmetrical wave ripples with flat tops. The crest lines are usually straight or slightly curved. Interference ripples or ladder back ripples (Fig. 5b) are present locally. Bidirectional and bipolar cross stratification is also present and indicates reversal of paleo-current direction. The fine-grained sandstone at Bandalamottu is characterized by plane beds with parting lineation, at places bidirectionally cross stratified and wave ripple laminated.

The sandstones are calcareous subfeldspathic arenites to quartz arenites with well-rounded quartz grains (Fig. 6a). Monocrystalline quartz dominates over polycrystalline quartz. Potash feldspar grains outnumber the plagioclase feldspar grains. Alteration of the plagioclase to a carbonate-sericite assemblage is more pronounced than kaolinitization of the potash feldspars. Tourmaline, zircon, and muscovite occur as minor components.

Different generations of cements with varied compositions are present in the sandstones. Authigenic overgrowth of potash feldspar is common (Fig. 6b) along with minor quartz overgrowth. Carbonate, silica, and sulfide cements have filled the available pore spaces in sandstones. Replacement of quartz grains by sulfide cements (Fig. 6a) is a common textural feature in sandstones.

The sandstone is followed upward by shale and dolomite successively. Shale contains abundant but thin sandstone partings. The upper dolomite is best developed at Bandalamottu but is absent at Dhukonda. The upper dolomite contains alternating light gray and pink bands. The pink dolomite bands contain microbial laminations and are locally stromatolitic. The dolomite is again followed upward by thick shale. A persistent 40-cm- to 2-m-thick magnetite-bearing banded chert layer (banded iron formation?) occurs within this top shale unit.

The depositional setting is interpreted to be mud-dominated one with intermittent sandstone and dolomite. Primary structural organization in the sandstone units, which include planar bed with parting lineation at the base; trough cross-stratification near the middle; and bidirectional (apparently bipolar) cross-stratification, interference ripples, and wave ripples near the top, are interpreted to indicate a marine peritidal environment (Klein 1975; Prothero and Schwab 1997). The wave ripples indicate deposition of the sediments above the fair weather wave base. Textural maturity of the sandstones also lends support to a nearshore platformal depositional setting. The microbially laminated dolomites are interpreted as intertidal deposits. Shale units in the study area do not contain any structures characteristic of exposure but are carbonaceous and pyritic. Such facies can be deposited from the suspension in the reducing low energy zone below the

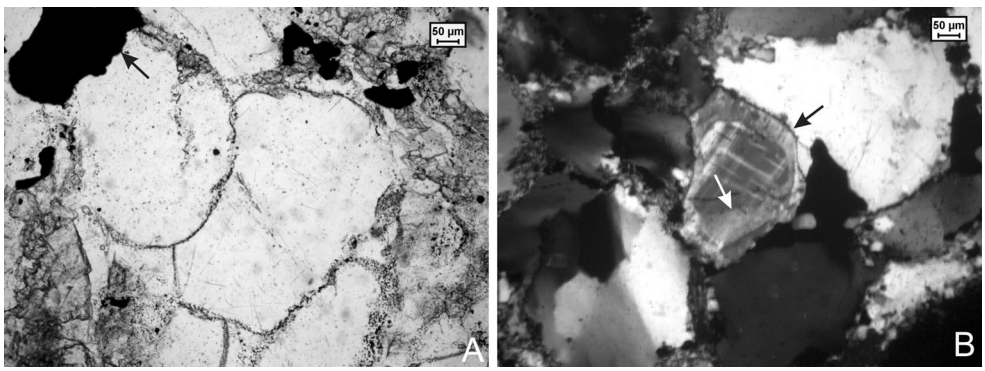

Fig. 6 Photomicrograph of mineralized Nallakonda sandstone. **a** Coarse-grained quartz arenite with well-rounded quartz grains. Grain boundaries are defined by early diagenetic ferruginous coatings. Note the corroded margin (arrow marked) of quartz grain developed due to replacement by sulfide (here chalcopyrite and bornite) cement (dark), Nallakonda deposit. **b** Subfeldspathic arenite showing potash feldspar overgrowth (dark arrow) on detrital potash feldspar grain (white arrow), Nallakonda deposit

effective wave base or mud line. This type of deposit is known to be associated with the carbonate layers and chert bands (Selley 2000). Some of the mudstones/shales, however, might have been deposited in shallower (intertidal) setting.

Mineralization

Nature of mineralization

The Agnigundala Sulfide Belt consists of three significant deposits at Dhukonda, Nallakonda, and Bandalamottu (Fig. 2a). Regional structural interpretations and stratigraphic correlation indicate that mineralization at the Nallakonda and Dhukonda occurs in sandstones and dolomite which forms the lower limb of a regionally developed westerly closing nappe structure (Fig. 3). At Bandalamottu, the mineralized horizon is deformed and participated in regional folding (Fig. 3). Sediment-hosted copper-lead deposits of the belt are characterized by several types of mineralization, which often grade from one type to another. These types include banded, disseminated, vein type, and breccia hosted. Copper mineralization at Nallakonda is confined to the carbonate-cemented sandstone and is stratabound and disseminated. Copper sulfides locally form irregular clots and/or thin veinlets.

Copper and lead sulfides at the Dhukonda deposit occur as disseminations within coarse-grained carbonate-cemented sandstone. Galena and minor chalcopyrite are also present within dolomite as fracture filling and/or replacement veins and locally as stringers along beddings in dolomite.

Dolomite hosts lead sulfide mineralization at Bandalamottu. Mineralization consists of stratabound, layer parallel veins (Fig. 7a) or breccias (Fig. 7b). The veins are zoned, from wall to the center: cherty bands followed by a pyrite-rich band and then by galena. Pure galena veins are also common. A major portion of the deposit occurs as breccia-fill where rectangular to irregular fragments of the dolomite float in a galena matrix. At places, gaps between breccia clasts are partially filled with well-developed crystals of ore-phase dolomite and galena (Fig. 7c). Ore-phase dolomite is variably replaced by galena (Fig. 7d).

Ore mineralogy and textures

Mineralogy of the ores of the Agnigundala Sulfide Belt is simple and includes bornite, chalcopyrite, pyrite, galena, sphalerite, cobaltite, and millerite with minor amount of sphalerite, x-bornite, yarrowite (Cu_9S_8), and spionkopite ($Cu_{1.4}S$).

Nallakonda deposit

Mineralization in carbonate-cemented sandstone of the Nallakonda deposit consists of fine-grained disseminations of cobaltite and copper sulfides within interstitial spaces between detrital and secondary (authigenic) phases (Fig. 8a), and their shape and volume are controlled by sedimentary/early

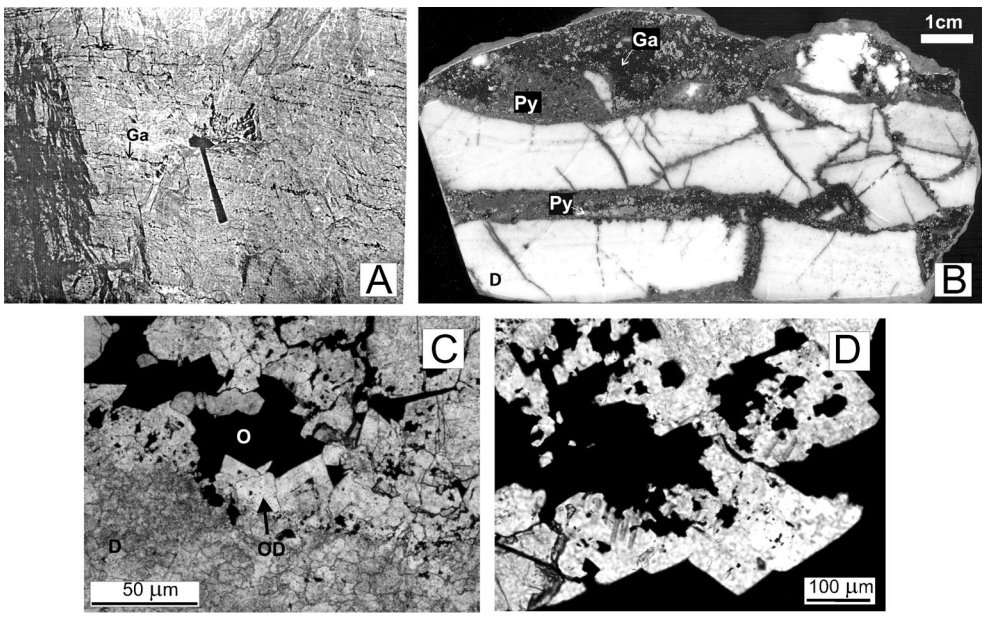

Fig. 7 **a** Photograph of layer parallel replacement vein-type ore mineralization in dolomite, underground of Dhukonda deposit. Hammer length 30.5 cm. **b** Photograph of polished hand specimen of breccia-filling ore in dolomite, Dhukonda deposit. The gaps in between dolomite fragments (D) are filled by galena and pyrite. Also note the replacement of dolomite by sulfides along the vein walls. **c** Photomicrograph (transmitted light) showing development of idiotopic ore-phase dolomite (OD) followed by sulfides (O), here galena, within the open spaces in brecciated dolomites, Bandalamottu deposit. **d** Photomicrograph (transmitted light) of ore-phase dolomite, variably replaced by galena (dark), Bandalamottu deposit

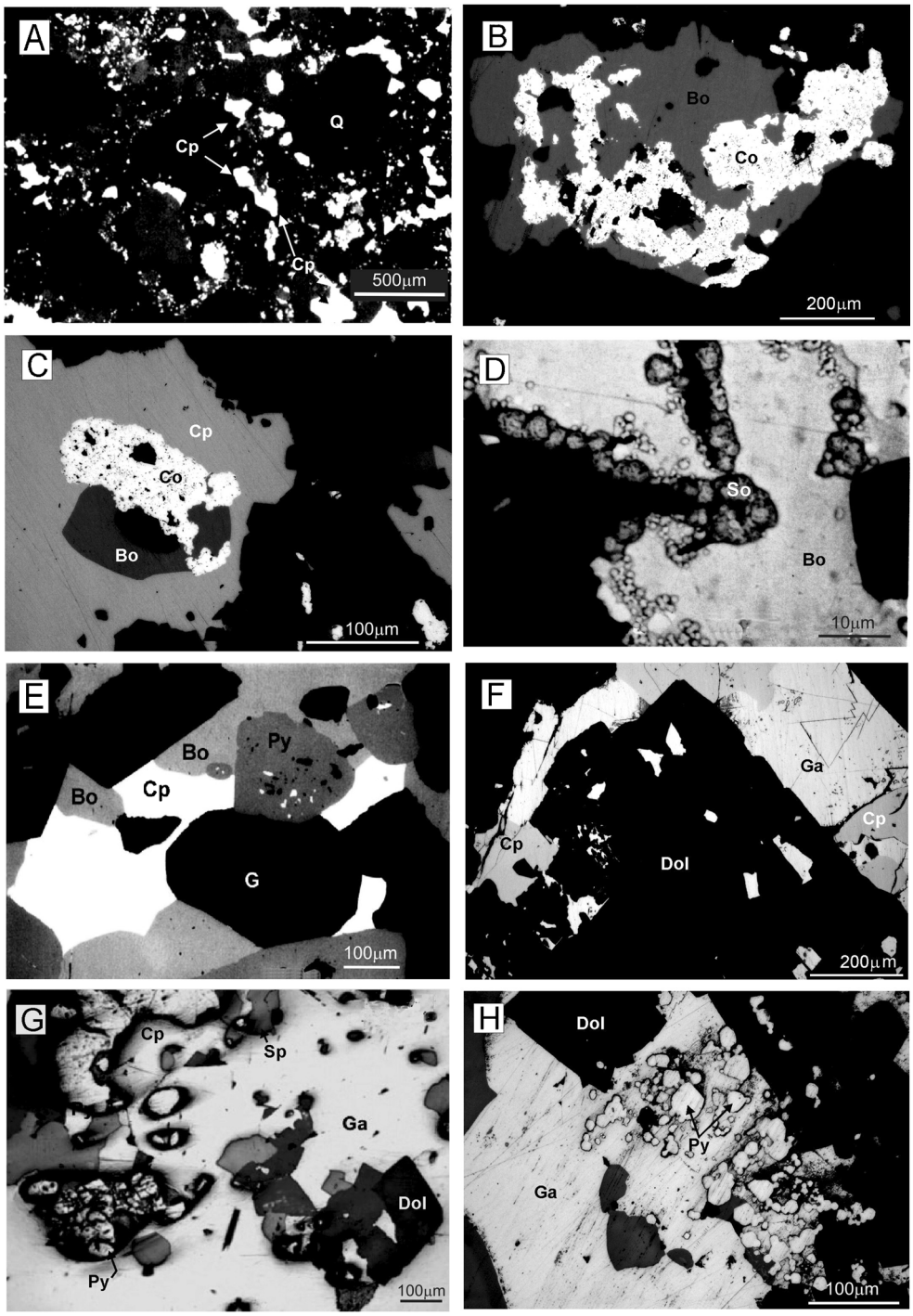

Fig. 8 **a** Photomicrograph showing chalcopyrite (Cp) as interstitial space filling cement in between quartz grains (marked Q) in sandstone, Nallakonda deposit. **b** Photomicrograph showing replacement of early cobaltite (Co) by bornite (Bo), Nallakonda deposit. **c** Photomicrograph showing mutual boundary relationship between chalcopyrite (Cp) and bornite (Bo), and both replacing early cobaltite (Co), Nallakonda deposit. **d** Fine-grained spionkopite (So) developed along the outer margin of bornite (Bn) grains, Nallakonda deposit. **e** BSE-SEM image showing textural equilibration between pyrite (Py), bornite (Bo), chalcopyrite (Cp), and gangue minerals (G) in a thicker ore vein, Nallakonda deposit. **f** Photomicrograph showing replacement of early ore-phase dolomite (Dol) by galena (Ga) and chalcopyrite (Py), Dhukonda deposit. **g** Photomicrograph showing massive aggregate of galena (Ga) containing sphalerite (Sp) and chalcopyrite (Cp) replacing early pyrites (Py) and gangue minerals (G), Dhukonda deposit. **h** Photomicrograph showing skeletal pyrites (Py) in a mosaic of galena grains (Ga), Bandalamottu deposit

diagenetic fabrics. A positive correlation exists between the size of detrital grains and the size and abundance of ore sulfide grains. Early-formed cobaltite is replaced by bornite and/or chalcopyrite (Fig. 8b). The bornite grains are intimately intergrown with chalcopyrite having mutual boundary relationships (Fig. 8c). Trace phases, including x-bornite, yarrowite, and spionkopite, occur as secondary minerals. Texturally, these minerals are confined along the margins of primary minerals; for example, x-bornite occurs at the margins of the bornite grains. Fine-grained yarrowite and spionkopite are either found along the outer margin of bornite grains (Fig. 8d) or are located at the contact between bornite and cobaltite.

Detrital grains, early-formed cements, and ore minerals have been replaced by late sulfides. Such replacement may lead to the development of massive sulfide with embedded relics of earlier corroded grains (Fig. 8e). Quartz, cupreous feldspar overgrowths, and carbonate cements are the major minerals that have been replaced by late sulfides. Authigenic

feldspars are considered as precursor of sulfide mineralization in several deposits the world over (Kucha 1985; Kucha and Pawlikowski 1986). A general sequence of mineralizing events is (1) quartz and feldspar authigenesis and carbonate cementation; (2) pre-ore cobaltite precipitation; (3) precipitation of bornite and chalcopyrite in available pore spaces; and (4) development of yarrowite and spionkopite through replacement of early-formed bornite and chalcopyrite.

Dhukonda deposit

The sulfide ores at the Dhukonda deposit occur in sandstone and dolomite. The copper-rich assemblage (chalcopyrite-bornite-cobaltite-pyrite galena-millerite) is present in the sandstone, whereas the lead-rich assemblage (galena-chalcopyrite) occurs in dolomite. Ore minerals are very fine grained and occur as disseminations and locally as massive aggregates or clots within the host rocks. Replacement of early dolomite by chalcopyrite and galena (Fig. 8f) produced massive replacement vein-type ores.

Euhedral to subhedral pyrite is present as disseminations throughout the deposit, and local pyrite-rich zones are present. Skeletal pyrite grains are replaced by later sulfide phases (Fig. 8g). Chalcopyrite occurs as interstitial fillings in sandstone or as chalcopyrite-rich zones developed through replacement of grains, cements, and early-formed pyrites. Galena occurs as anhedral polycrystalline aggregates within interstitial spaces in sandstone. Galena grains have replaced or included all other early-formed mineral phases.

Minor and trace minerals such as millerite are generally associated with chalcopyrite in sandstone and occur as anhedral granular masses or locally as massive aggregates. Other trace minerals like cobaltite, bornite, and sphalerite grains occur as fine- to very-fine-grained disseminations within chalcopyrite aggregate.

Replacement of detrital grains (quartz and feldspar), authigenic cements, and early ore minerals by the late phases leads to the development of massive mineralization with embedded relics of earlier corroded chalcopyrite, pyrite, rare sphalerite, and dolomite grains (Fig. 8g). Textural studies indicate the following mineralization sequence: (1) decomposition of feldspar was followed by silicate authigenesis and carbonate cementation; (2) precipitation of pre-ore pyrite; and (3) cobaltite-millerite, chalcopyrite, sphalerite, and galena precipitation.

Bandalamottu deposit

At Bandalamottu, galena and pyrite occur as fine-grained disseminations in the dolomite host. Galena aggregates in veins show a wide degree of recrystallization. Two generations of pyrite are present: early pyrite occurs as disseminations with skeletal form within a mosaic of galena crystals (Fig. 8h), and the late recrystallized euhedral pyrite grains may contain small galena inclusions. Trace minerals such as chalcopyrite and euhedral to anhedral sphalerite also occur as disseminations within a mosaic of galena crystals. A general sequence of mineralization events is (1) dolomitization and precipitation of pre-ore pyrite and (2) chalcopyrite, sphalerite, and galena deposition.

Ore mineral chemistry

Sampling and analytical techniques

The samples studied for ore mineral chemistry were collected from the Nallakonda, Dhukonda, and Bandalamottu deposits. Major element compositions of cobaltite, millerite, pyrite bornite, chalcopyrite, sphalerite, galena, yarrowite, and spionkopite were determined with a JEOL-JXA 733 EPMA at Hiroshima University, Japan. The instrument was operated with 15 kV accelerating voltage, 2–5 μm beam diameter, and 10 nA specimen current. Natural mineral standards were used and new analytical data were corrected by ZAF. The target grains of sulfide phases of polished blocks were analyzed for minor and trace elements using an Agilent HP-4500 quadrupole ICP-MS with UP-213 Nd:YAG laser probe (LA-ICP-MS) with beam resolution as low as 5 μm at the Centre for Ore Deposit Research (CODES) analytical facility, University of Tasmania, Australia. Single-point laser shots over a 100-s period created a crater 5–20 μm across and approximately 100 μm in depth. A synthetic standard was analyzed regularly after five spot analyses of the samples to check the accuracy (also see Maslennikov et al. 2009; Danyushevsky et al. 2011). The use of LA-ICP-MS technique yielded for the first time a more complete and precise elemental dataset (with accuracy of second decimal level) for the mineral phases of the Agnigundala Sulfide Belt. The results are presented in the ESM Tables 2A and 2B.

Results

Cobaltite is the only cobalt-rich phase in the Agnigundala Sulfide Belt and is present at the Nallakonda and Dhukonda deposits. Analyses of cobaltite from the Nallakonda deposit show enrichment of nickel, copper, selenium, molybdenum, silver, cadmium, antimony, gold, lead, and bismuth (ESM Tables 2A and 2B). Cobaltite grains from the Dhukonda deposit are nickel-rich compared to those from the Nallakonda deposit (ESM Tables 2A and 2B). Stoichiometric millerite is the sole nickel-bearing phase in the Dhukonda deposit. It contains cobalt as a major element and also copper and iron as minor elements.

Pyrite is abundant in the Dhukonda and Bandalamottu deposits but absent in the Nallakonda deposit. Early pyrite is enriched with germanium, selenium, cadmium, cobalt, nickel, arsenic, lead, and molybdenum. As vs. Co/Ni and Se vs. Co/Ni variation diagrams (Fig. 9a, b) show separate

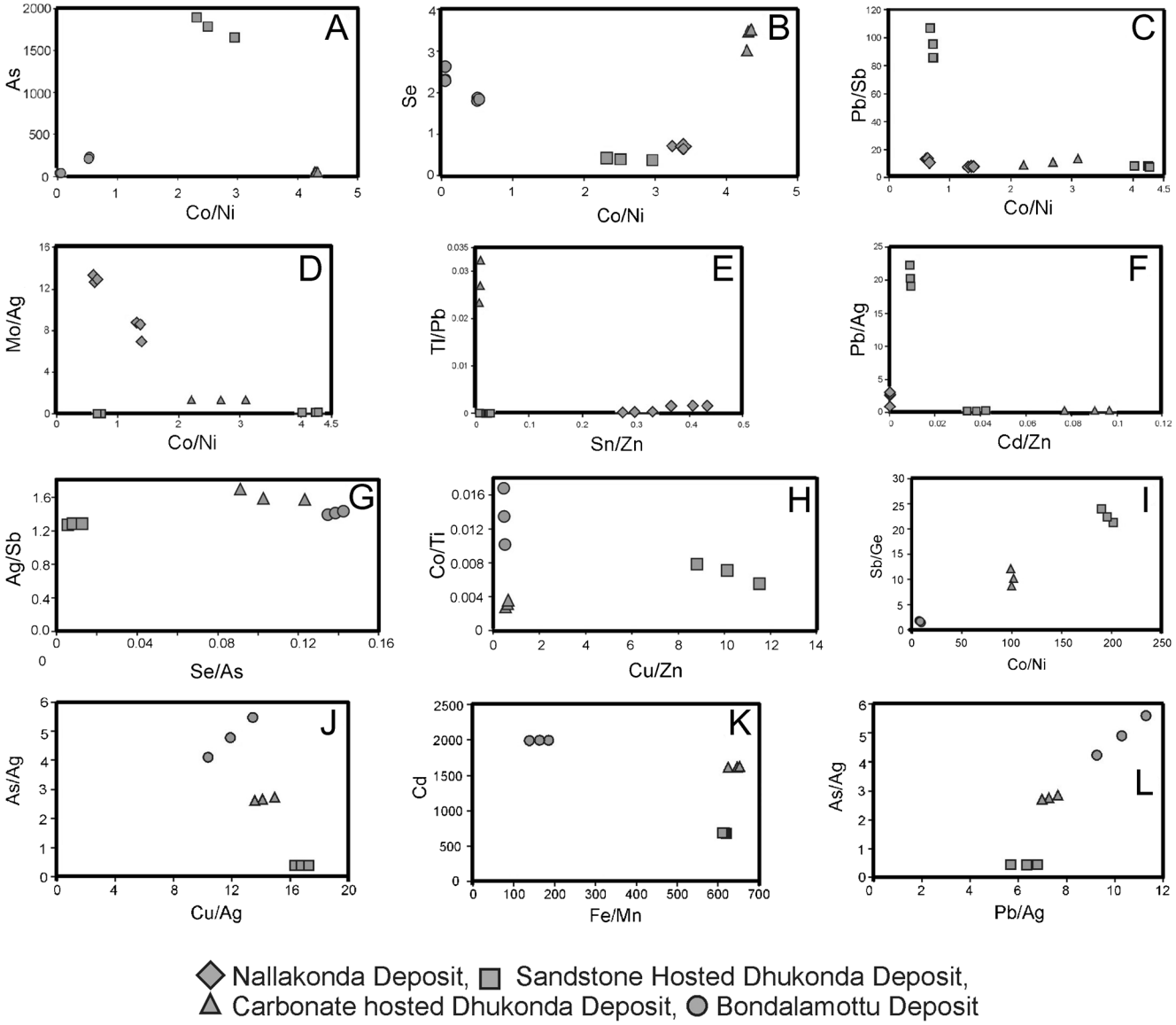

Fig. 9 Comparison of trace elements content in sulfide phases of Nallakonda, Dhukonda, and Bandalamottu deposits. **a** As vs. Co/Ni plots of pyrites of Dhukonda and Bandalamottu deposits show separate compositional fields. **b** Se vs. Co/Ni plots of cobaltites from Nallakonda deposit show similar trace element composition as pyrites from sandstone-hosted Dhukonda deposit. Carbonate-hosted Dhukonda and Bandalamottu deposits show separate compositional range. **c** Pb/Sb vs. Co/Ni plots and **d** Mo/Ag vs. Co/Ni plots of chalcopyrites from sandstone-hosted Dhukonda deposit show bimodal Co/Ni ratio and from carbonate-hosted Dhukonda deposit show intermediate values. **e** Tl/Pb vs. Sn/Zn and **f** Pb/Ag vs. Cd/Zn plots of chalcopyrite from Nallakonda and Dhukonda deposits show separate compositional range. **g** Ag/Sb vs. Se/As and **h** Co/Ti vs. Cu/Zn plots of galena from carbonate-hosted and sandstone-hosted Dhukonda deposit and carbonate-hosted Bandalamottu deposit showing distinct variations. **i** Sb/Ge vs. Co/Ni, **j** As/Ag vs. Co/Ag, **k** Cd vs. Fe/Mn, and **l** As/Ag vs. Pb/Ag plots of sphalerite from Dhukonda and Bandalamottu deposits, indicating different compositions of sphalerite from these two deposits. Trace element compositions of sphalerite from carbonate-hosted Dhukonda deposit are intermediate between sandstone-hosted Dhukonda deposit and Bandalamottu deposit

compositional field of pyrites from Dhukonda and Bandalamottu deposits. The Co/Ni ratio in pyrite from Dhukonda is comparable to that of the cobaltites from the Nallakonda deposit.

Bornite of the Nallakonda deposit is enriched in germanium, arsenic, selenium, molybdenum, silver, cadmium, tellurium, and bismuth. Some bornite from the Nallakonda and Dhukonda deposits is copper deficient and sulfur enriched.

Chalcopyrite, the most important copper sulfide, is present in all three deposits and enriched in germanium, arsenic, silver, antimony selenium, and tellurium. The Co/Ni ratio in chalcopyrite (Fig. 9c, d) from the sandstone-hosted Dhukonda deposit has a bimodal distribution. The lower values are similar to the chalcopyrite from the Nallakonda deposit, and the higher values resemble chalcopyrite from the carbonate-hosted Dhukonda deposit. Pb/Sb vs. Co/Ni,

Mo/Ag vs. Co/Ni, Tl/Pb vs. Sn/Zn, and Pb/Ag vs. Cd/Zn variation diagrams (Fig. 9c–f) indicate separate fields for chalcopyrite from the Nallakonda and Dhukonda deposits.

Galena grains from the Dhukonda and Bandalamottu deposits are rich in iron, selenium, bismuth, tellurium, silver, antimony, arsenic, and cadmium (ESM Table 2B). Ag/Sb vs. Se/As and Co/Ti vs. Cu/Zn variation diagrams (Fig. 9g, h) show distinct fields of galena from these two deposits.

Sphalerite from the Dhukonda and Bandalamottu deposits contains considerable iron but little Mn. Concentration of elements such as Co, Cu, Cd, Pb, Se, Te, Ge, As, and Ag is also high. Sb/Ge vs. Co/Ni, As/Ag vs. Cu/Ag, Cd vs. Fe/Mn, and As/Ag vs. Pb/Ag variation diagrams (Fig. 9i–l) separate sphalerites of the Dhukonda deposit from Bandalamottu deposits.

The Au content in the studied samples is very low (0.4–5 ppb). Chalcopyrite and bornite have very high Cu/Au ratios (ESM Table 2B). A somewhat higher value of Au is found in the Dhukonda and Bandalamottu deposits in sphalerite and pyrite, respectively, with relatively lower Cu/Au ratios. The values of Au are low and are comparable to the values (1–5 ppb) reported from several sediment-hosted Zn-Pb deposits (McGoldrick and Keays 1990) which are mostly indistinguishable from background values of host sedimentary rocks.

The S/Se ratios in the three deposits are large and vary from 88,000 to more than 6,500,000 (ESM Table 2 B). The selenium value varies from 0.01 to 3.5 ppm at Dhukonda, 0.37 to 2.1 ppm at Nallakonda, and 0.64 to 2.63 ppm at Bandalamottu.

The mineral chemistry of the sulfide phases of the Agnigundala Sulfide Belt indicates that the Cu-, Pb-, Zn-, and Fe-rich ore-fluid, which was responsible for the mineralization, had significant concentration of Co, Ni, As, Ge, Se, Mo, Ag, Cd, Bi, Sb, and Te.

Mineral and elemental zoning

Like other sediment-hosted base metal sulfide deposits, the Agnigundala Sulfide Belt also exhibits lateral and vertical mineralogical and elemental zoning. Mineralogically, the Agnigundala Sulfide Belt shows a lateral variation from rich in bornite, chalcopyrite, and cobaltite at Nallakonda to galena rich at Bandalamottu through chalcopyrite and galena rich at Dhukonda. The concentration of sphalerite in the Bandalamottu ore is comparatively higher than in the Dhukonda ores.

Apart from this lateral mineralogical zoning, individual deposits also display vertical mineralogical zoning. The Nallakonda deposit is bornite rich at the base and chalcopyrite rich near the top. In the Dhukonda deposit, the zoning is evident from the chalcopyrite-galena mineralization in sandstone and galena mineralization in overlying dolomite. The zoning at the Bandalamottu deposit is represented by the local enrichment of pyrite-chalcopyrite-sphalerite near the vein wall and galena-rich zone at the center of the veins. Similar zonation is present in many sediment-hosted sulfide deposits, including the Kupferschiefer (Oszczepalski 1999), Zambian Cu-belt (Garlic 1961), and northern Australian deposits (Large et al. 2005).

The minor and trace element chemistry of sulfide phases of the three deposits shows significant variations. Different variation diagrams show pronounced clustering of selected trace element ratio plots of sulfide phases of different deposits. There are differences in trace element concentrations of the same mineral of different deposits.

The As vs. Co/Ni diagram (Fig. 9a) for pyrite indicates a sharp drop in As content from sandstone-hosted deposit to the carbonate-hosted deposits. The Co/Ni ratio and Se value of cobaltite from the Nallakonda deposit are comparable to the Co/Ni ratio and Se value of pyrite from the sandstone-hosted Dhukonda deposit (Fig. 9b). The diagram also indicates that the Se value increases from the sandstone-hosted deposits to the carbonate-hosted deposits.

The Co/Ni ratio in chalcopyrite (Fig. 9c, d) from the sandstone-hosted Dhukonda deposit has bimodal clustering, where the lower values are similar to those of the Nallakonda deposit, and the higher values are comparable to the carbonate-hosted deposit. Pb/Sb ratios (Fig. 9c) in chalcopyrite are quite low in all the deposits with some exceptions from the sandstone-hosted Dhukonda deposit. The Mo/Ag ratio (Fig. 9d) in chalcopyrite drops from the Nallakonda deposit to the Dhukonda deposit. The Tl/Pb vs. Sn/Zn plot of chalcopyrite (Fig. 9e) indicates a decrease in Sn/Zn ratio from the Nallakonda deposit to the Dhukonda deposit. The Tl/Pb ratio is similar within all sandstone-hosted deposits but is higher in the carbonate-hosted deposits. The Cd/Zn ratio of chalcopyrite (Fig. 9f) increases from the Nallakonda deposit to the Dhukonda deposit. The ratio also increases from the sandstone-hosted deposit to the carbonate-hosted deposit at Dhukonda.

Variation diagrams for trace elements in galena indicate an increase in the Se/As ratio (Fig. 9g) but a decrease in the Cu/Zn ratio (Fig. 9h) from sandstone-hosted deposits to carbonate-hosted deposits. The Co/Ti (Fig. 9h) ratio is lower in the Dhukonda deposit than in the Bandalamottu deposit.

Variation diagrams of trace elements in sphalerite show a sympathetic drop in Co/Ni and Sb/Ge (Fig. 9i) ratios from the sandstone-hosted Dhukonda deposit to the carbonate-hosted Dhukonda deposit and finally to the Bandalamottu deposit. A drop in Cu/Ag ratio (Fig. 9j) is antipathetic to As/Ag ratio among the sandstone-hosted Dhukonda, carbonate-hosted Dhukonda, and Bandalamottu deposits. Fe/Mn ratios in sphalerites (Fig. 9k) are higher in the Dhukonda deposit than the Bandalamottu deposit, but Cd values are higher in the carbonate-hosted deposits. The Pb/Ag ratio increases with the increase of As/Ag ratio (Fig. 9l) in these deposits.

The comparative assessment of elemental variations in sulfide phases of the Nallakonda, Dhukonda, and Bandalamottu deposits reveals upward and lateral decrease in Cu, Co, Ni, As, and Mo contents and increase in Pb, Zn, Fe, Mn, Ag, Sb,

Cd, Te, Tl, and Ge contents. However, Sn and Te values show a reverse trend, lower in chalcopyrite of Nallakonda in comparison to Dhukonda.

Stable isotope geochemistry

Sulfur isotope geochemistry

Sampling and analytical technique

Nine monomineralic sulfide mineral separates of bornite, chalcopyrite, and galena were analyzed for sulfur isotopic compositions using a IR Laser combination VG Sira Series II mass spectrometer at Central Science Laboratory, University of Tasmania, Hobart, Australia. The results of the analysis are provided in ESM Table 3. Sample material was derived from the sandstone-hosted Nallakonda deposit and the carbonate-hosted Dhukonda and Bandalamottu deposits. Samples from Nallakonda include bornite and chalcopyrite from two different textural settings: one from the co-existing sulfides and another from where these two minerals do not coexist. Selected samples of chalcopyrite were also analyzed from the fine-grained ore of the Dhukonda deposit. Both fine-grained and recrystallized coarse-grained galenas were analyzed from the carbonate-hosted Dhukonda and Bandalamottu deposits.

Sulfide phases were obtained for analysis from thin films of the samples and then laser ablated for analysis, and other samples were collected using a dental drill for conventional analysis. The samples were converted to SO_2 gas by in vacuo reaction with CuO in a furnace, and the resulting gas mixture was purified by cryogenic removal of water and CO_2 following the methods of Robinson and Kusakabe (1975). The purified gas was frozen and flame sealed into 6-mm glass vials and subsequently analyzed. Commercially available bottled SO_2 gas was used as the working standard. The SO_2 working gas was calibrated using certified reference materials supplied by the International Atomic Energy Agency (IAEA). All S isotope values are expressed in the delta notation in ‰ (per mil) relative to V-CDT (Vienna-Canyon Diablo Troilite; Ault and Jensen 1963). The results have a one-sigma precision of ± 0.1‰.

Results

The $\delta^{34}S$ values of the chalcopyrite from the Nallakonda deposit are uniformly positive, but the values are more positive for the samples from Dhukonda deposit. The $\delta^{34}S$ values of bornite range from 3.2 to 3.8‰ (ESM Table 3). $\delta^{34}S$ values for fine-grained galena ores differ from the values of recrystallized ore for the samples from Dhukonda (ESM Table 3). The $\delta^{34}S$ value of the galena of the Bandalamottu deposit is the lowest (− 0.4‰) among the values obtained for the studied sulfide minerals. $\delta^{34}S$ values of chalcopyrite and fine-grained galena are heavier at the Dhukonda deposit compared to chalcopyrite from Nallakonda and galena from Bandalamottu.

Carbon-oxygen isotope geochemistry

Sampling and analytical technique

Carbon and oxygen isotope analyses of carbonates were carried out on samples collected from distal unmineralized dolomite, dolomite that occurs below the mineralized zone, and mineralized dolomite of the Dhukonda and Bandalamottu deposits. Carbonate cements of the Nallakonda deposit are also analyzed. Monomineralic carbonate separates were obtained from hand specimens using a dental drill to exclude contamination.

Analyses were carried out using a Micromass Optima mass spectrometer at Central Science Laboratory, University of Tasmania, Hobart, Australia. The crushed dolomite separates were left to react overnight with H_3PO_4 (18–25 h) at 50 °C following a technique modified after McCrea (1950). Excess H_2O and H_2S were then removed cryostatically and with a silver phosphate trap, respectively. The purified CO_2 gas was frozen and flame sealed into glass vials and subsequently analyzed on a mass spectrometer with a sequential multiport sample inlet system. A commercially available CO_2 bottle gas was used as a working standard, which was calibrated against internal laboratory standards included in each batch of samples.

Carbon isotope data are expressed in the delta notation in ‰ (per mil) relative to PDB (Peedee Formation, Belemnite; Urey 1947) and oxygen isotope data are in ‰ (per mil) relative to SMOW (Craig 1961). The O isotope results are recalculated in PDB scale using the relationship given by Dickson (1992), i.e., $\delta^{18}O_{PDB} = 0.97006 \times \delta^{18}O_{SMOW} - 29.94$.All data are listed in ESM Table 4. The results have a one-sigma precision of ± 0.1‰.

Results

Differences in O and C isotope composition are exhibited by mineralized and unmineralized dolomites. Two analyses of dolomites collected from the base of the mineralized zone exhibit distinctly different isotopic compositions: one is very similar to the dolomites that hosts lead mineralization and the other is more or less similar to unmineralized dolomite collected from an area much away from the mineralized zone.

It is interesting to note that lead-bearing dolomites from both Dhukonda and Bandalamottu plot in tight clusters with distinctly lighter $\delta^{18}O$ values and heavier $\delta^{13}C$ values than the unmineralized dolomites. Copper-bearing dolomite from Dhukonda shows markedly different isotopic composition with comparatively lighter $\delta^{18}O$ and $\delta^{13}C$ values. The isotopic composition of ore-stage carbonates at the Nallakonda deposit is very different to that of the earlier discussed dolomites as

both the $\delta^{13}C$ (−2.99 to −3.18‰) and $\delta^{18}O$ (−16.03 to −16.37‰) values are strongly lighter. The carbon and oxygen isotope signature becomes successively heavier from ore-stage carbonates at the Nallakonda deposit to copper-bearing dolomite at the Dhukonda deposit to lead-bearing dolomites at both the Dhukonda and Bandalamottu deposits.

Alteration

The mineralogy of the host sandstones and dolomite records readily recognizable mineral assemblages and textures which differ from mineral assemblages and texture of sandstones and dolomite of the same and different stratigraphic horizons exposed at a distance from the deposits. However, the change of mineral assemblages and texture between these sandstone and dolomite types could not be traced due to lack of exposures and drill cores. The ore zone sandstones contain, apart from coarse- to fine-grained quartz with sporadic silica overgrowth, potash feldspars with overgrowth of potash feldspars (Fig. 6b), sericite aggregates forming epi-matrix, and carbonate, silica, and sulfide phases as cements in pore spaces. The overgrown part of the potash feldspar shows increase in Cu/(Pb+Zn) and Fe/Mn ratios and in calcium content in comparison to the original grain (ESM Table 5). Replacement of grains and other cements by bornite, chalcopyrite, and galena is common (Fig. 6a). The sandstones exposed far away from the deposits lack overgrowth on potash feldspars, have little carbonate cement, and are devoid of sulfide cements. In these sandstones, sericitic alterations of potash feldspar are rare and silica cements are common. The grains of the host dolomite are cloudy with different shades of light brown and light gray, and there are patches of clear and white dolomite aggregates. The clear dolomite patches are discordant to the major fabric of the host dolomites. Such clear dolomite patches show close association with chalcopyrite and galena grains (Fig. 10a). Rhombic and clear dolomite that grew on pore walls shows nonreplacement grain boundaries with galena (Fig. 7c). In some locales, such rhombic dolomites are also replaced by galena (Fig. 7d). These textural relationships suggest that the clear late dolomites are ore-phase dolomite. The presence of quartz grains within the mosaic of light gray-brown dolomites is a common feature. Quartz-calcite veins are very common and a pervasive feature in mineralized dolomites. Aggregates of prismatic phlogopite are common constituents of the mineralized dolomite (Fig. 10b). These clear late dolomites with sulfide phases and aggregates of prismatic phlogopite are absent in dolomites exposed at a distance from the three deposits. Such mineralogical and textural attributes represent evidence in favor of wall rock alteration related to interaction between ore-fluid and host sediments.

Discussion

Hydrothermal fluids generated in sedimentary basins without active heating by coeval magmatism, like in the present case, are generally low temperature (< 200 °C) and oxidized (Lydon 2004; Cooke et al. 2000; Huston et al. 2006). At the same time, the absence of framboidal pyrite and primary nonstoichiometric copper sulfides in the ores of the studied belt also negates the possibility of a very low temperature of the ore-fluid (i.e., < 100 °C). In this context, the temperature of the ore-fluid of the present study was likely between 100 and 200 °C. Further, the Cu-Fe-S mineralogical (bornite → chalcopyrite → pyrite) and metal zonation (Cu → Pb±Zn) present in the Agnigundala Sulfide Belt was most likely caused by reduction of low-temperature oxidized fluid (see Brown 1971; Rose 1976; Kirkham 1989). Fluid inclusion homogenization temperatures from Bandalamottu (mean temperature of 277 °C, after Mishra and Mookherjee 1982 and Mishra 1985) are higher in temperature than inferred in the present study. Moreover, it is pertinent to note that the lack of chalcocite in the Nallakonda deposit suggests that the conditions were not overly oxidized; at the same time, the absence of pyrrhotite indicates the conditions were not that reduced. In this low-temperature system, deposition of bornite is followed by chalcopyrite and pyrite, and Pb (and Zn) deposition only occurs when sufficient H_2S becomes available (see Fig. 9 in Huston et al. 2016).

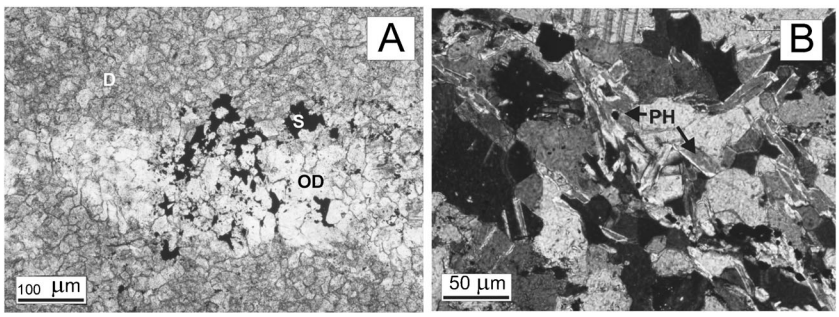

Fig. 10 **a** Photomicrograph showing two different types of dolomite. The ore-phase dolomite is clear and inclusion-free (marked OD), whereas the host dolomite (marked D) is dusty and contains abundant inclusions. Note ore-phase dolomites are associated with sulfide ore minerals (marked S). **b** Photomicrograph showing the presence of prismatic phlogopite (marked PH) in association with ore-phase dolomite

In the absence of syn-mineralization mafic magmatic rocks in the studied basin, the ore-fluid sulfate either came from trapped seawater from within the sedimentary basin or from evaporites present within the sedimentary succession (Kirkham 1989). This sulfate needs to be reduced to deposit copper-lead sulfides. Reduced sulfur can originate either by bacterial or by thermochemical reduction of seawater sulfate (Warren 2000). Average $\Delta_{SO4\text{-}sulfides}$ values of the studied samples vary from 17 to 11‰ (assuming an approximate $\delta^{34}S$ value of 17‰ for Proterozoic seawater), which fall well within the field of 10 to 20‰ for abiotic thermochemical sulfate reduction by organic compounds in the temperature range of 200 to 100 °C (Kiyosu and Krouse 1990; Hoefs 2009). For bacterial sulfate reduction, the fractionation values are much higher, between 15 and 60‰ (Goldhaber and Kaplan 1974; Ohmoto 1986; Machel et al. 1995). A biotic thermochemical sulfate reduction is consistent with the range and homogeneous $\delta^{34}S$ composition observed in this study. About 60 to 75% reduction of sulfate can produce the observed S isotope values (Fig. 11a). A relatively lower proportion of reduction gives lower values such as the $\delta^{34}S_{gn}$ value of 5.21 for the Dhukonda deposit and − 0.4 for the Bandalamottu deposit.

In an oxidized fluid, S and Se are well fractionated with an increase in the S/Se ratio (232,000 in modern seawater in contrast to 6000 for igneous rocks; Goldschmidt 1954). The studied sediments are intercalated with few pyroclastic layers, and convective circulation of basinal fluids through such pyroclastic layers may generate some sulfur, with a small range of $\delta^{34}S$ near to or slightly above 0‰, for the ore-fluid. However, the higher S/Se values (88,157 to more than 6,500,000) suggest paucity of Se in the source and match well with the values of seawater (Leutwein 1972; Stanton 1972) and, at the same time, stand against a significant contribution from intercalated pyroclastic layers or deep-seated basinal mafic flows.

Carbon-oxygen isotope signatures within ore-phase dolomites and calcite cements reflect changes in fluid composition and physicochemical conditions that prevailed during ore mineralization at the Agnigundala Sulfide Belt. Fractionation from a single fluid at constant temperature of 200 °C corresponds to a fluid with O isotopic composition that varies from

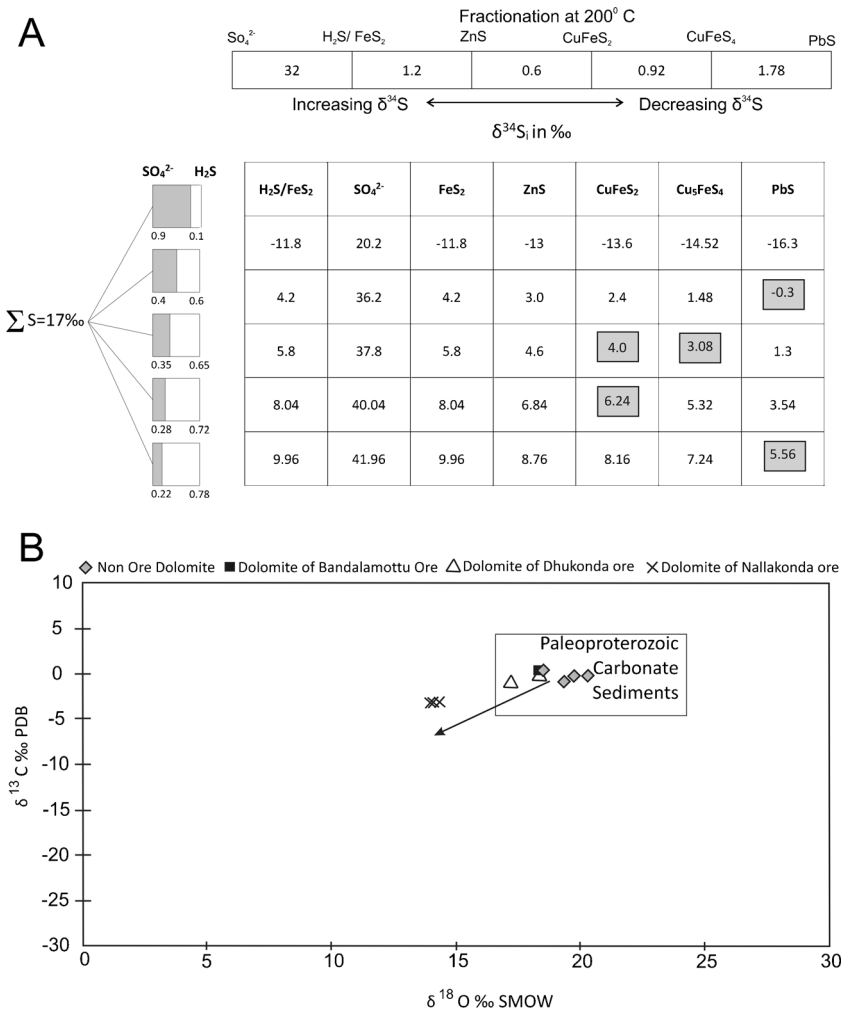

Fig. 11 **a** Sulfur isotope fractionation among sulfate, hydrogen sulfide, and sulfide minerals. The diagram was constructed for $T = 200$ °C and pH = 5.0 (in the presence of H_2S). The $\delta^{34}S$ of sulfide minerals varies according to the degree of sulfate reduction (for methodology, see Rye and Ohmoto 1974). The values in the gray fields match with the observed values. **b** Carbon-oxygen isotope data showing the difference between the ore-phase dolomites and regional sedimentary carbonates of Proterozoic age (after Large et al. 2001)

5.0 to 6.5‰ (ESM Table 4). The calculated $\delta^{18}O$ values are well within the range of basinal water (Taylor 1997). The $\delta^{18}O$ values likely have equilibrated with marine carbonate and other marine sediments having $\delta^{18}O$ values of − 9.0‰.

$\delta^{13}C$ and $\delta^{18}O$ values of host-rock dolomites from mineralized as well as unmineralized zones are consistent with published data for carbonates (Hudson 1977; Baker and Fallick 1989) and in particular for Proterozoic carbonates, i.e.,− 4.0 to + 4.0‰ for $\delta^{13}C$ and + 16 to + 28‰ for $\delta^{18}O$, respectively (Veizer and Hoefs 1976) (Fig. 11b). Both $\delta^{13}C$ and $\delta^{18}O$ isotope compositions become progressively lighter from unmineralized and Pb-Zn mineralized dolomites to copper mineralized carbonates in the Agnigundala Sulfide Belt. Similar trends (a vector indicating deviation from C-O isotopic ratios of unmineralized Proterozoic carbonates) are found in different skarn, MVT deposits, and sediment-hosted Pb-Zn deposits (Large et al. 2002, 2004; Selley et al. 2005; McGowan et al. 2006). The $\delta^{13}C$ and $\delta^{18}O$ values of calcite from the Nallakonda deposit are consistent with values obtained from MVT deposits (Richardson et al. 1998). Similarity in C-O isotopic ratios and their trend are indicative of a syn- to post-diagenetic replacement origin of the sulfide mineralization.

Carbonate is generated during thermochemical sulfate reduction of a sulfate-rich fluid (Machel 1987; Machel et al. 1995; Warren 2000). Such carbonates might have been precipitated as late hydrothermal calcites (also see McGowan et al. 2006). Lighter $\delta^{13}C$ and $\delta^{18}O$ values of calcite cement that occur in the interstitial spaces of mineralized sandstone at the Agnigundala Sulfide Belt may reflect an influx of carbonate species generated from oxidation and degradation of organic matter (methane in the present case). The calcite cement, related to mineralization, gives isotopic signatures more akin to the isotopic characters of hydrothermal fluid itself, whereas the C-O isotope values from dolomites are the products of dolomite recrystallization during hydrothermal fluid flow (also see Smith and Dorobek 1993; Nielsen et al. 1994).

The C isotope composition is much more affected by fluid-rock interaction than the O isotopic composition (Zheng and Hoefs 1990). Different temperatures of the mineralizing fluid may explain the observed O isotope signature in the Agnigundala Sulfide Belt, where the Nallakonda and Dhukonda Cu mineralization formed at higher temperature compared to the Pb mineralization of Dhukonda and Bandalamottu.

Alteration of host rocks is a common phenomenon in deposits formed from migrating ore-fluid (Evans 1993). Identification of the mineralization-related alteration pattern in sediment-hosted ore deposits sometimes becomes equivocal because burial diagenesis and greenschist facies metamorphism can produce similar mineral assemblages. However, the mineral assemblages such as overgrowth of potash feldspar on potash feldspar grains and development of late dolomite, calcite, and quartz cement along with phlogopite and sericite of host sandstones and dolomite, in contrast to their unmineralized counterparts, strongly advocates in favor of potassic, silica, and magnesium-calcium metasomatism under the influence of ore-fluids. Higher Cu, Fe, and Ca contents of the potash feldspar overgrowths and the close association of carbonate and silica cements with sulfide phases (Figs. 6a, b, 7c, d, and 10a, b) lend strong support to the fact that alteration of the host sediments is the result of interactions between ore-fluids and host rocks. This is also indicated by the change of C-O isotopic ratios from host dolomite to late carbonate cements.

The metal zoning, discussed above, largely reflects a thermal gradient across the studied ore district, similar to other well-studied VMS deposits (Lydon 2004). So, the Nallakonda copper deposit is definitely of higher temperature compared to the Dhukonda copper-zinc and Bandalamottu lead deposits. The presence of cobaltite and the enrichment of molybdenum also support a relatively higher formation temperature of the Nallakonda deposit.

Neither hematite nor pyrrhotite is present in the ore-stage assemblage which is within the pyrite stability field with log a_{O2} of >− 41 at 200 °C (ESM Fig. 1). Only higher temperature, reduced, acidic brines are capable of transporting gold together with copper, lead, and zinc. The observed low gold values in the studied ores, similar to several SEDEX deposits (McGoldrick and Keays 1990; Cooke et al. 2000), also support a low-temperature oxidized nature of the ore-fluid. Further, low manganese in the ores also supports the oxidized nature of the ore-fluid (see McGoldrick and Keays 1990).

Sedimentary rock-hosted stratiform base metal sulfide deposits are the product of basin- or subbasin-scale fluid flow systems. Such mineralization is the end product of processes involving a source(s) of metals and sulfur, metal transporting fluid, transport path, thermal or hydraulic pump, and physicochemical factors that result in ore precipitation (Leach et al. 2005; Selley et al. 2005; Hitzman et al. 2010). In this context, it can be envisaged that the lower red-bed and evaporite-bearing continental to shallow marine sediments, deposited during the syn-rift phase of basin evolution, might have supplied the metals to circulating sulfate-rich basinal fluids. The fluid was stored in the lower sedimentary succession under a cover of impervious shale of the shallow marine sedimentary succession of the post-rift phase. Rift-related faults developed during sedimentation in the basin might have punctured the ore-fluid pool in the lower geo-pressurized sedimentary succession and also acted as conduits for upward expulsion of an oxidized, low-temperature fluid. Intrabasinal ore-fluid flow took place through the sediments undergoing diagenesis from east to west under the pressure head that was developing in the east, which ultimately culminated in the form of a thrust along the eastern margin of the Cuddapah basin. The ore-fluid, under progressive cooling, deposited the copper sulfide ores at Nallakonda, copper-lead sulfide ores at Dhukonda, and lead sulfide ores at Bandalamottu. The ore-bearing horizons have participated in deformational events during basin inversion; however, those events failed to

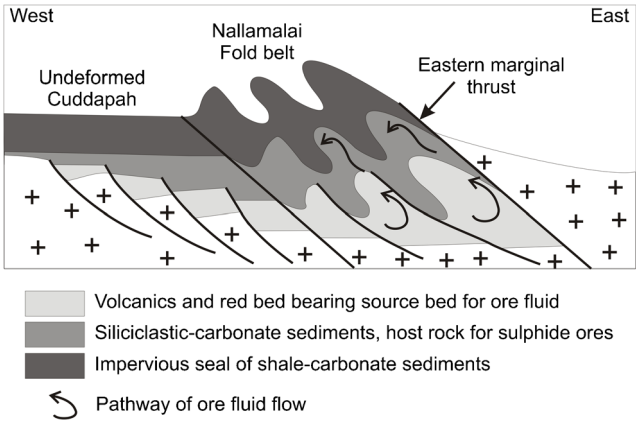

Fig. 12 A schematic genetic model for the studied ore mineralization showing the source rock, possible pathways of ore-fluid flow, and site of entrapment

impose any recognizable change in mineralization patterns. A schematic ore genetic model based on the outcome of the present study is shown in Fig. 12.

Summary

The Nallakonda copper deposit, Dhukonda copper-lead deposit, and Bandalamottu lead deposit in the Agnigundala Sulfide Belt occur in post-rift sediments that overlie early syn-rift sediments. Mineralogical and stable isotope systematics suggest that the ore-fluid was a low-temperature (< 200 °C) oxidized fluid. Stable isotope systematics of the sulfide phases suggest that the same ore-fluid which deposited copper at Nallakonda at relatively higher temperature also deposited copper-lead at Dhukonda and lead at Bandalamottu under progressive cooling during migration through sediments. The required sulfur was derived through thermochemical reduction of basinal water sulfate, and the metals were scavenged from the lower red-beds with evaporite-bearing continental to shallow marine sediments. Syn-sedimentary faulting caused puncturing of the ore brine pool and migration of the ore-fluid through the cover syn-rift sediments undergoing diagenesis. The mineralized horizons participated in deformation without registering any recognizable change in mineralization patterns.

Acknowledgements The first author is grateful to Prof. Ross Large, Ex-Director of CODES, Tasmania University, Australia, for extending a visitorship and allowing him to utilize the laboratory facilities. He is also thankful to Dr. P. McGoldrick and Dr. S. Bull for their valuable discussions and suggestions. The first author also expresses sincere thanks to Christine Cook of Central Science Laboratory, University of Tasmania and Sarah Gilbert of CODES, University of Tasmania, for their help in C, O, and S isotopes and LA-ICP-MS data generation. The authors are thankful to Dr. M Fukuoka of Hiroshima University, Japan, for EPMA analysis. The authors express their sincere thanks to Dr. B. Lehmann, Editor-in-Chief, *Mineralium Deposita*, Dr. D. L. Huston, Geoscience Australia and Associate Editor, *Mineralium Deposita*, and the other anonymous reviewer for their painstaking reviews, which have definitely improved the clarity of the manuscript.

References

Annels AE (1989) Ore genesis in the Zambian copper belt, with particular reference to the northern sector of the Chambishi Basin. In: Boyle RW, Brown AC, Jefferson, CW, Jowett EC, Kirkham RV (eds) Sediment-hosted stratiform copper deposits. Geol Assoc Can Spec Pap 36:427–452

Ault WV, Jensen ML (1963) Summary of sulfur isotope standards. In Jensen, M.L. (ed) Biochemistry of sulfur isotopes. National Science Foundation. Symposium Proceedings, Yale University

Baker AJ, Fallick AE (1989) Evidence from Lewisian limestones for isotopically heavy carbon in two-thousand-million-year-old sea water. Nature 337:352–354

Bhattacharya HN, Bull S (2010) Tectono-sedimentary setting of the Paleoproterozoic Zawar Pb-Zn deposits, Rajasthan, India. Precambrian Res 177:323–338

Blake DH, Stewart AJ (1992) Stratigraphic and tectonic framework, Mount Isa Inlier. In: Stewart AJ, Blake DH (eds) Detailed studies of the Mount Isa Inlier. AGSO Bull 243:1–11

Brown AC (1971) Zoning in the White Pine copper deposit, Ontonagon County, Michigan. Econ Geol 66:543–573

Brown AC (1974) An epigenetic origin for stratiform Cu-Pb-Zn sulfides in the lower Nonesuch Shale, White Pine, Michigan. Econ Geol 69: 271–274

Brown AC (1978) Stratiform copper deposits—evidence for their post-sedimentary origin. Miner Sci Eng 10:172–181

Chatterjee A, Bandopadhyay S, Bhattacharya HN (2000) Progressive development of structures in a ductile shear zone along a part of the eastern margin of Cuddapah basin, India. Indian J Earth Sci 27:33–39

Chaudhuri AK, Saha D, Deb GK, Patranabis Deb S, Mukherjee MK, Ghosh G (2002) The Purana basins of southern cratonic province of India—a case for Mesoproterozoic fossil rifts. Gondwana Res 5: 23–33

Collins AS, Patranabis-Deb S, Alexander E, Bertram CN, Falster GM, Gore RJ, Mackintosh J, Dhang PC, Saha D, Payne JL, Jourdan F, Backe G, Halverson GP, Wade BP (2015) Detrital mineral age, radiogenic isotopic stratigraphy and tectonic significance of the Cuddapah Basin, India. Gondwana Res 28:1294–1309

Cooke DR, Bull W, Large RR, McGoldrick PJ (2000) The importance of oxidized brines for the formation of Australian Proterozoic stratiform sediment-hosted Pb-Zn (SEDEX) deposits. Econ Geol 95:1–18

Craig H (1961) Isotopic variations in meteoric waters. Science 133:1702–1703

Crawford AR, Compston W (1973) The age of the Cuddapah and Kurnool systems, South India. J Geol Soc Aust 19:453–464

Danyushevsky LV, Robinson P, Gilbert S, Norman M, Large R, McGoldrick P, Shelley JMG (2011) A technique for routine quantitative multi-element analysis of sulfide minerals by laser ablation ICP–MS. Geochem Explor Environ Anal 11:51–60

Dickson T (1992) Carbonate mineralogy and chemistry. In: Tucker ME, Wright VP (eds) Carbonate sedimentology. Blackwell Science Ltd., Hong Kong, pp 284–313

Evans AM (1993) Ore geology and industrial minerals an introduction, 3rd ed. Blackwell Science Ltd., Singapore, p 389

Garlick WG (1961) The syngenetic theory. In: Medelsohn F (ed) The geology of the northern Rhodesian Copper Belt. MacDonald, London, pp 146–162

Goldhaber MB, Kaplan IR (1974) The sedimentary sulfur cycle. In: Goldberg EB (ed) The sea, vol 4. Wiley, New York

Goldschmidt VM (1954) Geochemistry. Clarendon. 730 pp

Goodfellow WD (2004) Geology, genesis and exploration of SEDEX deposits, with emphasis on the Selwyn Basin, Canada. In: Deb M, Goodfellow WD (eds) Sediment-hosted lead-zinc sulfide deposits. Narosa Publishing House, New Delhi, pp 24–99

Hitzman MW, Kirkham R, Broughton D, Thorson J, Selley D (2005) The sediment-hosted stratiform copper ore system. In: Hedenquist JW, Thompson JFH, Goldfarb RJ, Richards JP (eds) Economic geology 100th anniversary volume. Society of Economic Geologists, Inc., Colorado, pp 609–642

Hitzman MW, Selley D, Bull S (2010) Formation of sedimentary rock-hosted stratiform copper deposits through earth history. Econ Geol 105:627–639

Hoefs J (2009) Stable isotope geochemistry, 6th edn. Springer, Berlin 293 pp

Hudson JD (1977) Stable isotopes and limestone lithification. J Geol Soc Lond 133:637–660

Huston DL, Stevens B, Southgate PN, Muhling P, Wyborn L (2006) Australian Zn–Pb–Ag ore-forming systems: a review and analysis. Econ Geol 101:1117–1158

Huston DL, Mernagh TP, Steffen G, Hagemann SG, Doublier MP, Fiorentini M, Champion DC, Jaques AL, Czarnota K, Cayley R, Skirroe R, Bastrakov E (2016) Tectono-metallogenic systems—the place of mineral systems within tectonic evolution, with an emphasis on Australian examples. Ore Geol Rev 76:168–210

Kaila KL, Tewari HC (1982) Structure and tectonics of the Cuddapah basin in the light of DSS studies. In: Bhattacharji S, Balakrishna S (eds) Evolution of the Intracratonic Cuddapah Basin. Institution of Indian Peninsular Geology Monograph 2, Hyderabad, pp 53–62

Kaila KL, Tewari HC (1985) Structural trends in the Cuddapah Basin from deep seismic sounding and their tectonic implication. Tectonophys 115:69–86

Kaila KL, Roy Chowdhury K, Reddy PK, Krishna VK, Narain M, Sublotin SI, Sollogub VB, Chekhunov AV, Kharetchko TV (1979) Crustal structure along the Kavali Udipi profile in the Indian peninsular shield from deep seismic sounding. J Geol Soc India 20:307–333

Kirkham RV (1989) Distribution, settings and genesis of sediment-hosted stratiform copper deposits. Geol Assoc of Can Spec Pap 36:3–38

Kiyosu Y, Krouse HR (1990) The role of organic acid in the abiogenic reduction of sulfate and the sulfur isotope effect. Geochim J 24:21–27

Klein GV (1975) Paleotidal range sequence, Middle Member, Wood Canyon Formation (Late Precambrian), eastern California and western Nevada. In: Ginsburg RN (ed) Tidal deposits. Springer, New York, pp 171–177

Kucha H (1985) Felspar, clay, organic and carbonate receptors of heavy metals in Zechstein deposits (Kupferschiefer type), Poland. Tran Inst Min Metall Sect B Appl Earth Sci:133–146

Kucha H, Pawlikowski M (1986) Two-brine model of the genesis of strata-bound Zechstein deposits (Kupferschiefer type), Poland. Mineral Deposita 21:70–80

Lakshminarayana G, Bhattacharjee S, Ramanaidu KV (2001) Sedimentation and stratigraphic framework in the Cuddapah basin. Geol Surv India Spec Publ 55:31–58

Large RR, Bull SW, Winefield PR (2001) Carbon and oxygen isotope halo in carbonates related to the McArthur River (HYC) Zn-Pb-Ag deposit; implications for sedimentation, ore genesis and mineral exploration. Econ Geol 96:1567–1593

Large RR, Bull S, Selley D, Yang J, Cooke D, Garven G, McGoldrick P (2002) Controls on the formation of giant stratiform sediment-hosted Zn-Pb-Ag deposits: with particular reference to the north Australian Proterozoic. In: Cooke DR, Pongratz J (eds) Giant ore deposits: characteristics, genesis and exploration. CODES spec Publ 4, pp 107–149

Large R, McGoldrick P, Bull S, Cooke D (2004) Proterozoic stratiform sediment-hosted zinc-lead-silver deposits of northern Australia. In: Deb M, Goodfellow WD (eds) Sediment-hosted lead zinc sulfide deposits. Narosa Publishing House, New Delhi, pp 1–23

Large RR, Bull SW, McGoldrick PJ, Walters S (2005) Stratiform and strata-bound Zn-Pb-Ag deposits in Proterozoic sedimentary basins, northern Australia. Ecron Geol 100th Anniversary Volume, pp 931–963

Leach DL, Sangster DF, Kelley KD, Large RR, Garven G, Allen C, Gutzmer J, Walters S (2005) Sediment-hosted lead-zinc deposits: a global perspective. In: Hedenquist JW, Thompson JFH, Goldfarb RJ, Richards JP (eds) Econ Geol 100th Anniversary Volume, pp 561–607

Leutwein F (1972) Selenium. In: Wedepohl H (ed) Handbook of geochemistry. Springer, New York 34-B-!-34-O-1

Lydon JW (2004) Genetic models for Sullivan and other SEDEX deposits. In: Deb M, Goodfellow WD (eds) Sediment-hosted lead-zinc sulfide deposits. Narosa Publishing House, New Delhi, pp 149–190

Machel HG (1987) Saddle dolomite as a by-product of chemical compaction and thermochemical sulfate reduction. Geology 15:936–940

Machel HG, Krouse HR, Sassen R (1995) Products and distinguishing criteria of bacterial and thermochemical sulfate reduction. Appl Geochem 10:373–389

Maslennikov VV, Maslennikova SP, Large RR, Danyushevsky LV (2009) Study of trace element zonation in vent chimneys from the Silurian Yaman-Kasy volcanic-hosted massive sulfide deposit (Southern Urals, Russia) using laser ablation-inductively coupled plasma mass spectrometry (LA-ICPMS). Econ Geol 104:1111–1141

McCrea JM (1950) On the isotopic chemistry of carbonates and paleotemperature scale. J Chem Phys 18:844–857

McGoldrick PJ, Keays RR (1990) Mount Isa copper and lead-zinc-silver ores: coincidence or cogenesis? Econ Geol 85:641–650

McGowan RR, Roberts S, Foster RP, Boyce AJ, Coller D (2003) Origin of the copper-cobalt deposits of the Zambian Copper Belt: an epigenetic view from Nchanga. Geology 31:497–500

McGowan RR, Roberts S, Boyce AJ (2006) Origin of the Nchanga copper-cobalt deposits of the Zambian Copper Belt. Mineral Deposita 40:617–638

Meijerink AMJ, Rao DP, Rupke J (1984) Stratigraphic and structural development of the Precambrian Cuddapah Basin, SE India. Precambrian Res 26:57–104

Mishra B (1985) Ore petrology and geochemistry of three Proterozoic carbonate-hosted sulfide deposits from India. Unpublished Ph.D. thesis, Indian Institute of Technology, Kharagpur, 364 pp

Mishra B, Mookherjee A (1982) Preliminary studies on fluid inclusion geothermometry of quartz-sulfide veins from Zawar area, Rajasthan, using a heating stage with kanthol strips. Proc National workshop on fluid inclusion studies in minerals, IIT, Bombay, pp 20–30

Nagaraja Rao BK, Rajurkar ST, Ramalingaswamy G, Ravindra Babu B (1987) Stratigraphy, structure and evolution of the Cuddapah basin. Geol Soc India Mem 6:33–86

Narayanswami S (1966) Tectonics of the Cuddapah basin. J Geol Soc India 7:33–50

Nielsen P, Swennen R, Keppens E (1994) Multiple-step recrystallization within massive ancient dolomite units: an example from the Dinantian of Belgium. Sedimentology 41:567–584

O'Dea MG, Lister GS (1997) Geodynamic evolution of the Proterozoic Mount Isa terrain, orogeny through time. In: Burg JP, Ford M (eds) Geol Soc Spec Publ 121:99–102

Ohmoto H (1986) Stable isotope geochemistry of ore deposits. In: Valley JW, Taylor HP, O'Neil JR (eds) Stable isotopes in high temperature geological processes. Rev in Mineral 16:491–559

Oszczepalski S (1999) Origin of the Kupferschiefer polymetallic mineralization in Poland. Mineral Deposita 34:599–613

Phansalkar VG, Kale AS, Karmalkar NR, Kale VS (1991) An unusual evaporate association from the Papaghni Group, Cuddapah Basin. J Geol Soc India 37:75–79

Piranjo F (2000) Ore deposits and mantle plume. Kluwer Academic, Dordrecht, p 556

Plimer IR (1986) Sediment-hosted exhalative Pb-Zn deposits; products of contrasting ensialic rifting. Trans Geol Soc S Afr 89:57–73

Plumb KA, Ahmad M, Wygralak AS, (1990) Mid-Proterozoic basins of the North Australian Craton-regional geology and mineralisation. In: Hughes FE (ed) Geology of the mineral deposits of Australia and Papua New Guinea, Melbourne. Aust Inst Min Metall 881–902

Prothero DR, Schwab F (1997) An introduction to sedimentary rocks and stratigraphy. W.H. Freeman, 575 pp

Richardson CK, Rye RO, Wasserman MD (1998) The chemical and thermal evolution of the fluids in the cave-in-rock fluorspar district, Illinois: stable isotope systematics at the Deardroff mine. Econ Geol 83:765–783

Robinson BW, Kusakabe M (1975) Quantitative preparation of SO_2 for $^{34}S/^{32}S$ analyses, from sulfides by combustion with cuprous oxide. Anal Chem 47:1179–1181

Rose AW (1976) The effect of cuprous chloride complexes in the origin of red bed copper and related deposits. Econ Geol 71:1036–1048

Rye RO, Ohmoto H (1974) Sulfur and carbon isotopes and ore genesis: a review. Econ Geol 69:826–842

Saha D (2002) Multi stage deformation in the Nallamalai Fold Belt, Cuddapah Basin, South India—implications for Mesoproterozoic tectonism along the south-eastern margin of India. Gondwana Res 5:701–719

Saha D, Chakraborty S (2003) Deformation pattern in the Kurnool and Nallamalai Groups in the north-eastern parts (Palnad area) of the Cuddapah basin, South India and its implications on Rodinia/Gondwana tectonics. Gondwana Res 6:573–583

Sarkar SC, Gupta A (2012) Crustal evolution and metallogeny in India. Cambridge University Press, New York, p 840

Sawkins FJ (1989) Anorogenic felsic magmatism, rift sedimentation and giant Proterozoic Pb-Zn deposits. Geology 17:657–660

Selley RC (2000) Applied sedimentology, 2nd edn. Academic, San Diego 523 pp

Selley D, Broughton D, Scott R, Hitzman M, Bull S, Large R, McGoldrick P, Croaker M, Pollington N, Barra F (2005) A new look at the geology of the Zambian copper belt. Econ Geol 100th Anniversary Volume, pp 965–1000

Sivadas KM, Sashikumar KT, Subba Rao N, Setti DN, Rajurkar ST, Sharma RK, Gopalkrishnan KP, Sagar AK, Ziauddin M, Murthy YG, Narayanswamy S (1985) Lead and copper deposits of the Agnigundala mineralized belt, Guntur district, Andhra Pradesh. Geol Surv India Mem 118:102

Smith TM, Dorobek SL (1993) Alteration of early-formed dolomite during shallow to deep burial: Mississippian Mission Canyon Formation, central to south-western Montana. Geol Soc Am Bull 105:1389–1399

Stanton RL (1972) Ore petrology. McGraw-Hill, New York 713 **pp**

Sweeney MA, Turner P, Vaughan DJ (1986) Stable isotope and geochemical studies of the role of early diagenesis in ore formation, Konkola Basin, Zambian Copper belt. Econ Geol 81:1836–1852

Taylor HP (1997) Oxygen and hydrogen isotope relationships in hydrothermal mineral deposits. In: Barnes HL (ed) Geochemistry of hydrothermal ore deposits. Wiley, New York, pp 229–302

Unrug R (1988) Mineralization controls and source of metals in the Lufilian fold belt, Shaba (Zaire), Zambia, and Angola. Econ Geol 83:1247–1258

Urey HC (1947) The thermodynamic properties of isotopic substances. J Chem Soc (London), Part I 0:562–581

Veizer J, Hoefs J (1976) The nature of $^{18}O/^{16}O$ and $^{13}C/^{12}C$ secular trends in sedimentary carbonate rocks. Geochim Cosmochim Acta 40: 1387–1395

Volodin RN, Chchetkin VS, Bogdanov Yu V, Narkelyun LF, Trubachev AI (1994) The Udokan cupriferous sandstone deposit (eastern Siberia). Geol Ore Deposits 36:1–25

Warren JK (2000) Evaporites, brines and base metals: low-temperature ore emplacement controlled by evaporite diagenesis. Aust J Earth Sci 30:179–208

Zheng YF, Hoefs J (1990) Carbon and oxygen isotopic covariations in hydrothermal calcites, theoretical modeling on mixing processes and application to Pb-Zn deposits in the Harz Mountains, Germany. Mineral Deposita 28:79–89